Check for updates

Fresh emplacement of hydrated sodium chloride on Ceres from ascending salty fluids

M. C. De Sanctis[1]✉, E. Ammannito[2], A. Raponi[1], A. Frigeri[1], M. Ferrari[1], F. G. Carrozzo[1], M. Ciarniello[1], M. Formisano[1], B. Rousseau[1], F. Tosi[1], F. Zambon[1], C. A. Raymond[3] and C. T. Russell[4]

The surface and internal structure of Ceres show evidence of a global process of aqueous alteration, indicating the existence of an ocean in the past. However, it is not clear whether part of this ocean is still present and whether residual fluids are still circulating in the dwarf planet. These fluids may be exposed in a geologically young surface, and the most promising site to verify the occurrence of present fluids on Ceres is Cerealia Facula dome, in Occator crater. This very young facula exhibits minerals that are relatively rare in our Solar System, the formation of which requires the presence of liquid water in combination with hydrothermal activity. Here we report the discovery of hydrated sodium chloride on Cerealia Facula. These newly identified chloride salts are concentrated on the top of the dome, close to a system of radial fractures. The spatial distribution of the hydrated phase suggests that chloride salts are the solid residue of deep brines that reached the surface only recently, or are still ascending. These salts are very efficient in maintaining Ceres's warm internal temperature and lowering the eutectic temperature of the brines, in which case ascending salty fluids may exist in Ceres today.

Data returned by Dawn's mission found that Ceres appears to be sculpted by the action of water[1–5], indicating the presence of substantial subsurface ice[6–8] and isolated surface ice exposures[9,10]. Ahuna Mons and other domical mountains have been interpreted as the expression of potential cryovolcanism[11–13]. Similarly, cryovolcanism was suggested as a possible explanation of the sporadic observations of water emission from Ceres[14]. The Dawn data also provided evidence of a global process of aqueous alteration[15,16], indicating the presence of an ocean in the past history of Ceres. However, it is not clear whether part of this ocean is still present as a leftover and whether residual fluids are still circulating in its interior.

Cerealia Facula in Occator crater (Fig. 1 and Extended Data Fig. 1) is the most prominent bright feature associated with recent water activity[1–3] and is located in the central pit of Occator crater, which also hosts the Cerealia Tholus dome at its centre (Methods and Fig. 2). Cerealia Tholus dome (Fig. 2) is characterized by a series of radial fractures off-centred from the highest topographic point. The distal part and the boundary where Cerealia Facula fades into the surrounding terrains feature a series of concentric fractures, interrupted by an isolated, very bright, topographic high (Pasola Facula, Extended Data Fig. 2). Both the concentric and the radial fractures show the morphology of extensional fault system[17].

The formation of Occator central pit and tholus, as well as the emplacement of this very recent bright material, is debated[1,2]. Among the different hypotheses, the two major ones[1,2,18] are: (1) the formation and extrusion of liquid salty water induced by the heating due to Occator impact, which does not imply the pre-existing circulation of fluids at depth; and (2) the presence of pre-existing fluids due to endogenic processes, with ascending cryomagmas, facilitated by the fractures and conduits formed consequently to the impact.

The detailed study of the composition and distribution of the materials in Cerealia Facula can constrain the formation mechanisms of the minerals as well as the characteristics of the Cerean fluids from which such minerals are derived.

The Dawn Visible and Infrared Mapping Spectrometer (VIR)[19] data returned during the nominal phase indicated that the young bright facula exhibits minerals that are relatively rare in our Solar System. The formation of these minerals, mainly sodium carbonates and ammonium bicarbonate[2] or ammonium chlorides[2,3], requires the presence of liquid water in combination with hydrothermal activity. However, the data coverage and the resolution were not sufficient to fully understand the bright facula composition, the emplacement mechanism and the relation to the presence of subsurface fluids. The data of the Dawn second extended mission phase, acquired at very high resolution, are essential to disentangle the different emplacement hypotheses and to determine the circulation of the suggested subsurface fluids.

Mineralogical composition of Cerealia Facula

During the nominal operational phase of the Dawn mission[4], the VIR instrument mapped the mineral distribution over the Occator crater with a nominal spatial resolution of ~100 m pix^{-1}, showing a general increase in the abundance of the carbonates and ammonium salts towards the centre of Cerealia Facula[2,3]. Later, the high-resolution data acquired in the extended orbital phase provided a unique and extraordinary view of Cerealia (Fig. 1a), with a spatial resolution along the slit up to ~10 m.

This high spatial resolution, even if the coverage is limited across Cerealia Facula, enables the evaluation of the spectral differences within the bright material (Fig. 1b,c). The spectra clearly show changes in the level of reflectance, spectral slopes, depths of the different absorptions, and shape and structure of the broad and large

[1]Istituto di Astrofisica e Planetologia Spaziali, Istituto Nazionale di Astrofisica, Rome, Italy. [2]Agenzia Spaziale Italiana, Rome, Italy. [3]Jet Propulsion Laboratory, California Institute of Technology, Pasadena, CA, USA. [4]Earth Planetary and Space Sciences, University of California, Los Angeles, Los Angeles, CA, USA. ✉e-mail: mariacristina.desanctis@inaf.it
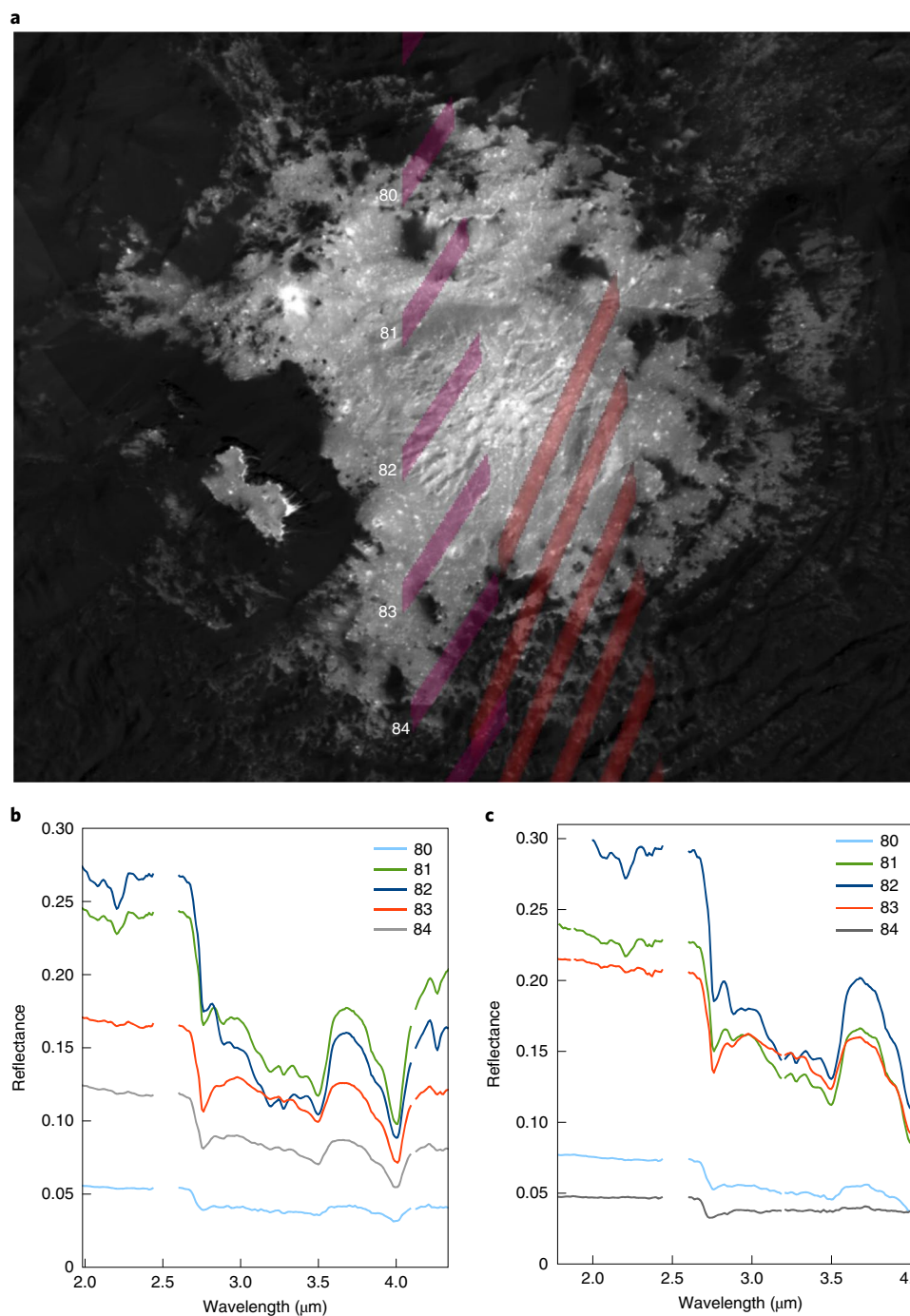
Fig. 1 | Cerealia Facula. a, Projections of the VIR lines on Occator (pink: VIR_IR_1B_1_582998159; red: VIR_IR_1B_1_584957323). The numbers indicate the lines in the data image. **b,c**, Spectra of different areas from VIR_IR_1B_1_582998159. Lines (80–84) go from north to south as shown in **a**. Lines 81, 82 and 83 are the closest to the dome centre. The spectra are averages of four contiguous pixels: pixels 16–20 (**b**) and pixels 61–64 in (**c**). Data between 2.45 and 2.55 μm have been removed due to a known instrument artefact.

band between 2.6 and 3.7 μm, where several minima at 2.76, 2.88, 3.2, 3.28, 3.38 and 3.49 μm are visible (Extended Data Fig. 3). Some spectra also show small minima near 2.96 and 3.1 μm. The minima at 2.76 μm have been previously ascribed to phyllosilicates and the minima at ~3.38 and ~3.49 μm to carbonates[2]; the minima at 2.88, 3.2 and 3.28 μm were observed in the previous data but not assigned to specific species. Analysis of the band depth demonstrates that the pixels closer to the dome peak generally show stronger bands at 2.2, 3.2, 3.28, 3.38, 3.49 and 4.0 μm (Fig. 1b,c). However, the correlations

between the carbonate band depth at 4.0 μm and the bands at 2.2, 3.2 and 3.28 μm are not linear (Fig. 3a).

While an overall increase in the band intensity is visible going towards the dome, the pixels closer to the dome peak show a stronger 2.2 μm band that does not correspond to a similar increase in the carbonate band (Fig. 3a). Similarly, the band intensities at 4.0 μm and at 3.2 μm and 3.28 μm, do not correlate linearly. Oppositely, the bands at 2.2 μm and 3.2 μm (not shown here) and 3.28 μm show a clear correlation (Fig. 3b), indicating that either the specie carrier of
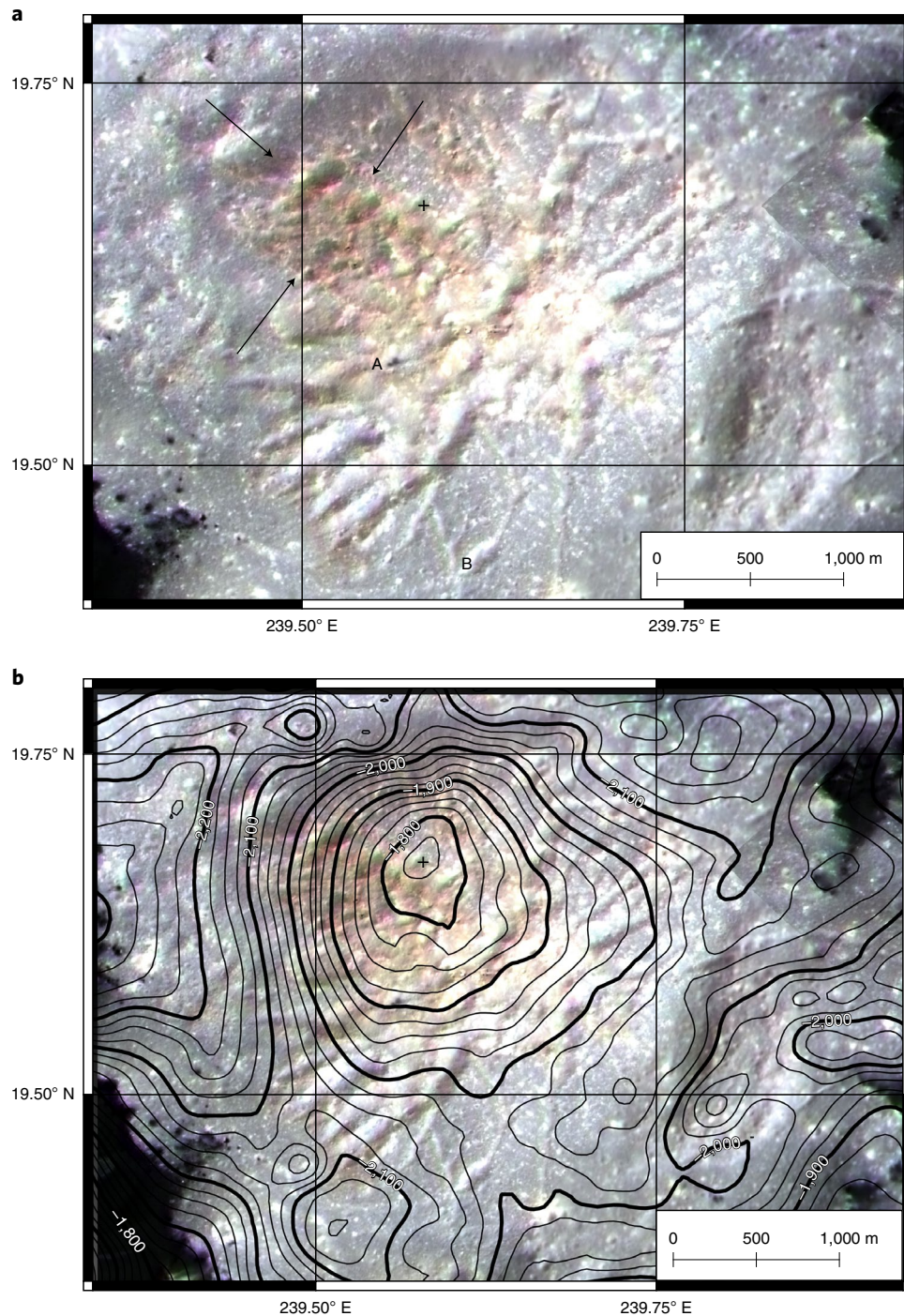
a

b

Fig. 2 | Morphology and colours of Cerealia Tholus. a, Pan-sharpened FC colour data ($R = 750$ nm, $G = 920$ nm, $B = 980$ nm). The two locations from where the blue (A) and orange (B) spectra in Fig. 1b were obtained are shown. Arrows indicate the densely fractured area located next to the peak and along the northwestern flank of Cerealia Tholus. The cross symbol indicates the position of the topographic peak of the tholus. **b**, Pan-sharpened FC colour controlled mosaic with the topographic isolines computed as elevation over the best-fit ellipsoid (semiaxis $a = 482$ km, semiaxis $b = 446$ km) of Ceres's shape. Thin isolines are spaced 25 m. The isolines show the asymmetrical shape of the tholus. The topographic peak of the tholus (black cross) is offset from the concentric fracture pattern on Cerealia.

the bands is the same or that these bands are due to different species linked to each other. The band at about 2.2 μm has been previously assigned to ammonium salts (NH_4 carbonate or NH_4 chloride) with better results using the NH_4 chloride in the spectral modelling[2,3].

To highlight spectral differences between different areas, here we make use of spectral ratios: the ratio enhances the signature of

the components that are present or more abundant in one area with respect to another.

The spectral ratio (Fig. 4) between areas close to the peak and on the flank (A and B in Fig. 2a) shows the band at 2.2 μm as well as a large, strong and structured band between 2.76 and 3.7 μm; the carbonate band is almost absent, suggesting that the carbonate content
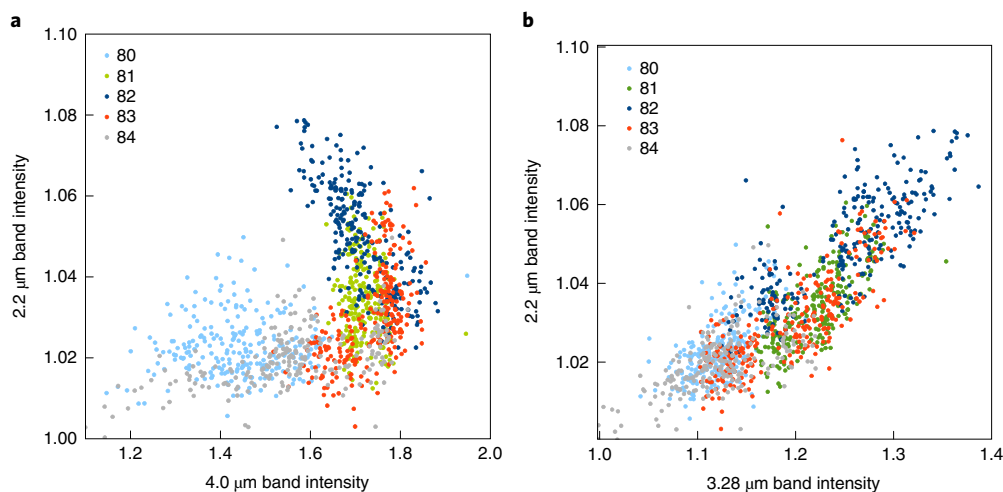
Fig. 3 | Band intensity. a, Plot of 2.2 µm versus 4.0 µm bands. **b**, Plot of 2.2 µm versus 3.28 µm bands. The colours of the points indicate the lines in the data (as in Fig. 1a); green, blue and orange are the pixels closer to the dome centre. The band intensity has been calculated using the band ratios between the band centres and the left shoulders as a proxy of the intensity.
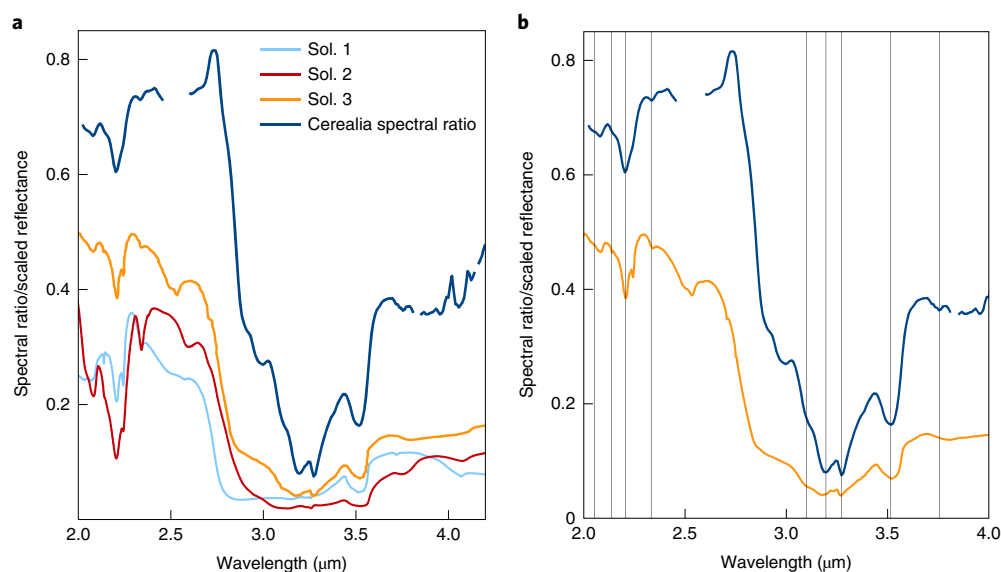

Fig. 4 | Cerealia spectral ratio compared with laboratory spectra of brines. a, Blue: ratio of spectra close to dome peak (A on Fig. 2a) and on the flank (B in Fig. 2a). Yellow: spectrum of Sol. 3 (a mixture of NH_4Cl, Na_2CO_3 and $NaCl \cdot 2H_2O$ (hydrohalite)). Red: spectrum of Sol. 2 (a mixture of NH_4Cl, NH_4HCO_3 and Na_2CO_3). Cyan: spectrum of Sol. 1 (a mixture of NH_4Cl and Na_2CO_3). **b**, Comparison of the spectral ratio and Sol. 3. The thin vertical lines highlight the features common between the two.

is nearly equal in the two areas under investigation. The spectral ratio demonstrates that the peak of the facula contains different proportions of the identified species and additional components, likely associated with the ammonium salt. Moreover, the overall shape of the spectral ratio, with the presence of a strong band around 3 µm, indicates the probable presence of hydration.

We used the already identified species, including ammonium salts (Extended Data Fig. 7), to fit the spectra of some areas on Cerealia, but the spectral modelling fails in reproducing the strong bands at 3.2 and 3.28 µm (Fig. 5a), implying that there are additional components not yet considered in the spectral mixture.

Hydrated sodium carbonates have been detected elsewhere on Ceres close to areas rich in anhydrous sodium carbonates and water ice[20]. Modelling the spectra of the Cerealia areas showing the strongest 2.76–3.7 µm band using hydrated sodium carbonate (Extended

Data Fig. 7) improves the overall fit but still fails in reproducing the 2.76–3.7 µm band (Fig. 5b). As a consequence, other species could be present in the mixture of minerals that constitutes the bright facula.

Laboratory studies on the freezing of fluids containing sodium, ammonium, carbonate and chloride ions reveal that different compositions are obtained depending on the proportions of the ions in solution and thermodynamical conditions[21,22]. In case of slow freezing, the mixtures form preferentially sodium-bearing species, in particular, hydrohalite ($NaCl \cdot 2H_2O$)[21]. Fast frozen brines form predominantly ammonium chloride and ammonium bicarbonate, but hydrohalite is formed when sodium and chloride were present in excess in the solutions[22] (Extended Data Fig. 8). In this case, the brine (hereafter called Sol. 3) is a mixture of NH_4Cl (ammonium chloride), Na_2CO_3 (natrite) and $NaCl \cdot 2H_2O$ (hydrohalite). In case of
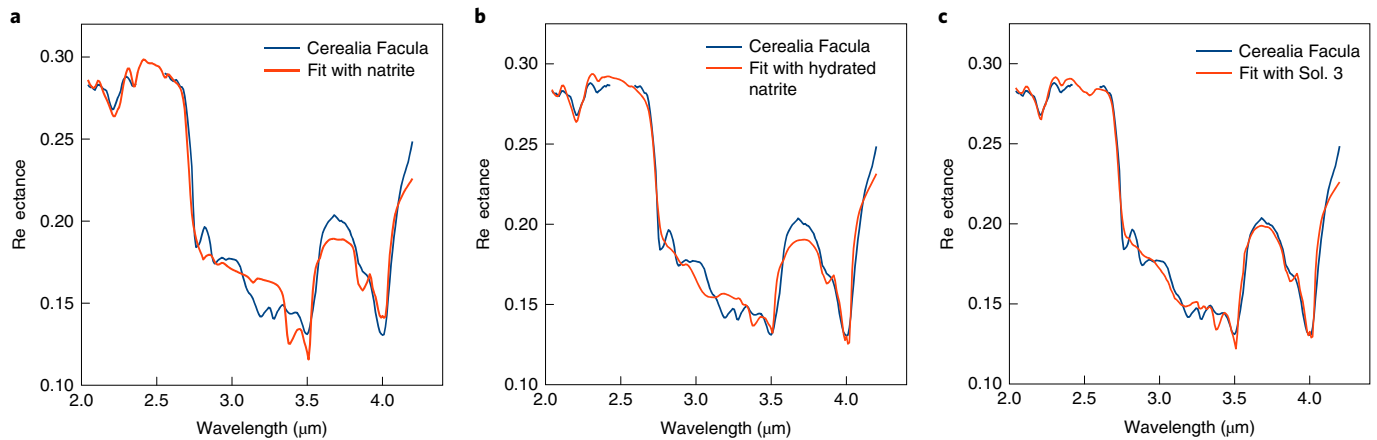
Fig. 5 | Spectral fits of the pixels in area A using different mixtures. a, Spectral fit with species previously identified in Cerealia Facula (natrite, NH$_4$Cl, illite, dark material, $\chi^2 = 5.08$) (refs. [2,3]). **b**, Spectral fit using also hydrated sodium carbonate (trona, natrite, dolomite, NH$_4$Cl, illite, dark material, $\chi^2 = 2.67$); **c**, Fit using Sol. 3 (Sol. 3, natrite, dolomite, NH$_4$Cl, illite, dark material, $\chi^2 = 1.57$). The abundance of the species used in the modelling are reported in Extended Data Fig. 7. The values of χ^2 diminish with the increasing goodness of the fits from **a** to **c**.

equimolar sodium and ammonium ions, the brine (Sol. 1) contains NH$_4$Cl, NH$_4$HCO$_3$ and Na$_2$CO$_3$, while in case of dominant ammonium and chloride, the brine (Sol. 2) is composed of NH$_4$Cl and Na$_2$CO$_3$.

The spectrum of Sol. 3 is remarkably similar to the spectral ratio of some areas of Cerealia Facula (Fig. 4), while the spectra of brines not containing hydrohalite (Sol. 1 and Sol. 2), do not look like the Cerealia spectral ratio (Fig. 4a).

To check for the presence of hydrohalite, we fit the Cerealia Facula spectrum adding Sol. 3, containing hydrohalite (Fig. 5c). The results indicate that the mixture with Sol. 3 strongly improves the fit, indicating that such brine is present on Cerealia.

The distribution of Sol. 3 and of the other components has been mapped using the retrieved abundances from the spectral modelling of the data on Cerealia dome (Fig. 6).

The spectral maps indicate that both sodium carbonate and Sol. 3 are present on Cerealia Tholus, but the two species are distributed differently (Fig. 6). The abundance of the sodium carbonate is lower on the top of the dome tholus (Fig. 6c,d) with respect the areas at its bottom, whereas the maximum quantity of Sol. 3 is located at the top of the dome tholus (Fig. 6a,b) and on its northwestern flank, which is considerably steeper than the other sides. The plots of the abundances versus elevation show clear trends of the two species (Fig. 6b,d), with the abundance of Sol. 3 (Fig. 6b) that nicely correlates with the elevation.

The spectra of the isolated Pasola Facula are also rich in carbonate and Sol. 3, but less with respect to the amount present on the dome. However, a few spectra collected on its southern part (Extended Data Fig. 4) are characterized by a broad not well-structured band at about 3 μm, suggestive of strong hydration in the area. The spectra correspond to an area showing, below a top coat of bright/grey material, a layer of extremely bright material from which landslides flow down, covering dark material (Extended Data Fig. 2). We cannot exclude that this very bright layer is the origin of the hydration seen in the spectra.

The way in which the bright material was emplaced and evolved suggests different reservoirs and/or origin, offering a window into the subsurface chemistry of Ceres. The main hypotheses include material originating from crustal brine pockets[23], from brines in the crust/mantle transition region[24] or from a shallow melt chamber locally created by the Occator impact[18]. The setting of Cerealia Facula in a central pit suggests that impact-induced processes must have played an important role in its formation. However, if the dif-

ferent species constituting the bright material were emplaced at the same time and then aged with time, we would expect a more uniform distribution of their abundances, while we clearly note an association of the brine containing hydrohalite with the peak of the dome (Fig. 6). Moreover, Cerealia Facula was formed at least 18 million years ago (Ma) after the formation of Occator crater[25] while the modelling of the impact-produced melt chamber suggests complete freezing after ~5 Ma (ref. [18]), implying a discrepancy between the cooling timescales of an impact-induced cryomagma chamber and the Cerealia Facula formation.

The concentration of hyrdrohalite is maximum at the topographic peak of the tholus where fractures are particularly dense, but offset from the centre of the radial fracture pattern. This suggests that successive distinct episodes have emplaced brines of different relative abundance on the surface of Occator's central dome. Models of cooling of the deep reservoir[24] indicate that eutectic temperatures for different solutions would have been reached at diverse times, resulting in a differentiated crystallization. Brines dominated by NaHCO$_3$ would have been the first to crystallize, but such brines would not extrude on the surface, being instead limited to shallower levels in the subsurface[24]. Further cooling of the reservoir would cause an enrichment in ice and sodium carbonate. The latest brine to freeze would contain sodium chloride (hydrohalite) and/or ammonium salts and would have been present in the reservoir for the longest periods of time, contributing to late manifestations of cryovolcanism[24]. As a consequence, the identification of hydrohalite in Cerealia Facula and its concentration on the peak of the dome could indicate recent episodes of cryovolcanism with extrusion of hydrated salt rich brines.

Hydration–dehydration equilibrium curves indicate the stability of hydrated salts in the presence of ice and dehydration of salts after sublimation of ice. To estimate the dehydration rate of hydrohalite on Cerealia, we adapted the ice sublimation model[26] described in Methods, substituting the ice thermal characteristics with those of hydrohalite, when available[5,26]. The thermophysical model was computed using the real topography of Occator. We calculate the rate of dehydration by using the classical formula for the sublimation of ice because the stability curve of hydrohalite with respect to dehydration at the conditions of Ceres's surface is similar to that of pure ice[27].

Thus, the dehydration rate of pure hydrohalite is predicted to be about one order of magnitude lower than that of water-ice sublimation.
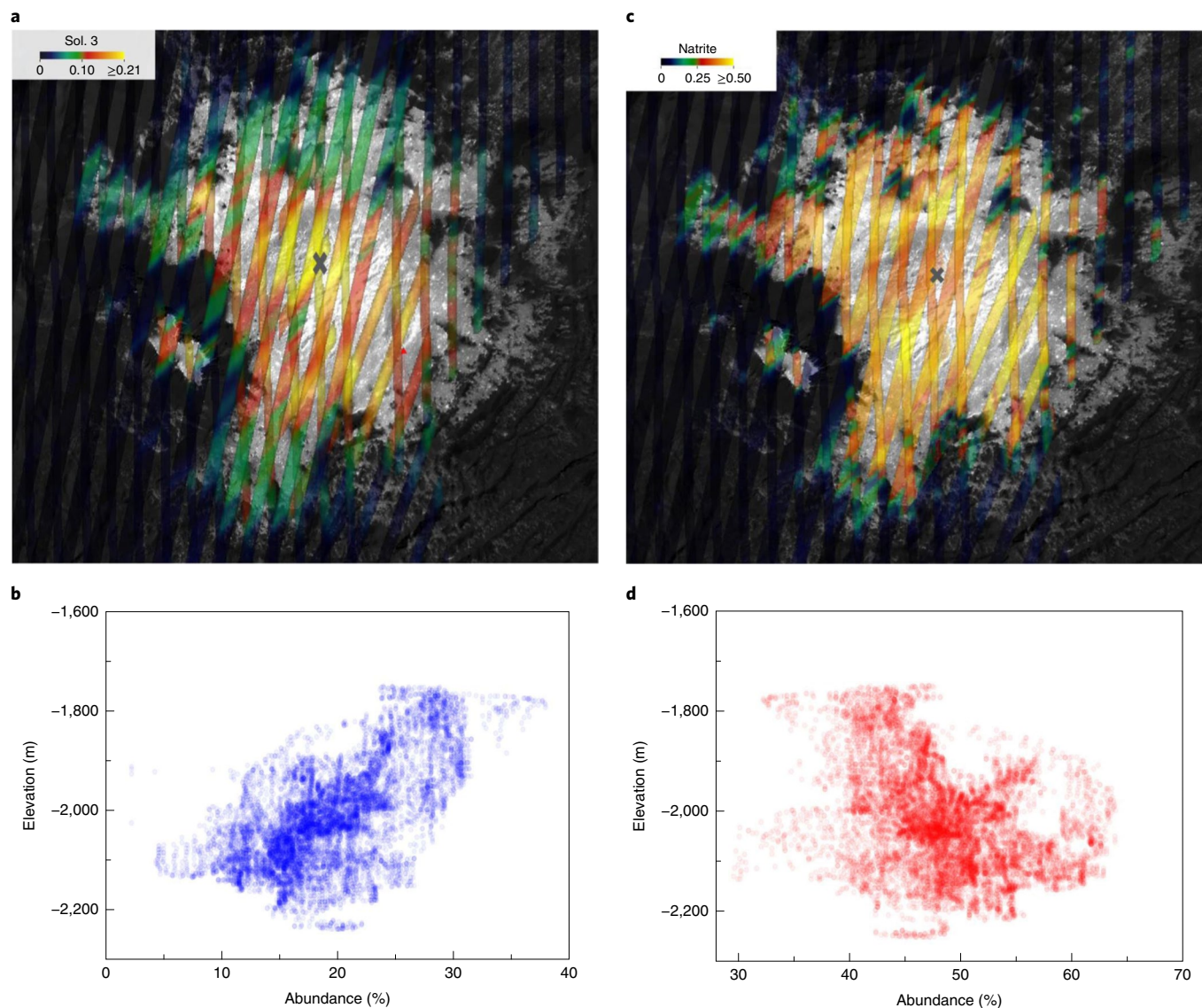
Fig. 6 | Brines on Cerealia Facula. a, Distribution of the retrieved abundance of Sol. 3. **b**, Plot of the retrieved abundance of Sol. 3 versus topography. **c**, Distribution of the retrieved abundance of natrite (Na_2CO_3). **d**, Plot of the retrieved abundance of natrite versus topography. Topography is computed as elevation over the best-fit ellipsoid ($a = 482\,km$, $b = 446\,km$) of Ceres's shape. The cross indicates the topographic peak of the tholus.

The results indicate that hydrohalite is unstable on the Ceres's surface and that it dehydrates in halite (NaCl), a specie featureless in the VIR spectral range, on a timescale of the order of 10^2 yr, if no source of hydration is provided (Methods). Two hypothesis can be drawn to maintain hydrated sodium chloride on the surface: (1) the presence of water ice in contact with the salts; and (2) recent/continuous refurbishment of hydrate brines from subsurface reservoirs.

Water ice has been observed elsewhere on Ceres's surface[9,10], but always in shadows or in close proximity to them, where the cold temperatures preserve the ice from rapid sublimation. The topography of Occator, and specifically the region where we observe the hydration, does not present long-lasting shadows. Moreover, we were not able to firmly identify water ice in the spectra of the central bright facula, implying that surficial water ice is not abundant at the VIR pixel scale.

Thus, the hydration state of the identified NaCl can be due to very recent or continuous emplacement, implying that brines would still be able to extrude on Ceres's surface. This scenario has been suggested by cooling modelling, if the fractures/conduits containing

the brines are able to maintain high enough ascending rates to transport them to the surface[24]. The facula shows concentric fractures on its distal boundary, associated with the collapse of the central pit, and radial fractures within the Cerealia Tholus, which are the expression of the uplift stress. These extensional fractures represent the preferable conduits where fluids can escape towards the surface.

On the icy satellites, subsurface liquids in conduits may be transported to the surface[28]. Even though the thermophysical conditions and processes are very different on Enceladus, sodium salts (NaCl, $NaHCO_3$ and/or Na_2CO_3) like those identified in Cerealia Facula have been detected in Enceladus's plume[29]. The plume also contains ice grains, simple organics[30,31] and complex macromolecular organic material[32], originating from an alkaline subsurface ocean.

Given the analogy of the minerals present in Cerealia and those identified in Enceladus's plume, we wonder whether organic material can be likewise present in Cerealia Facula. Indeed, aliphatic organics have been reported at specific locations (Ernutet region) on Ceres[33,34], in association with some materials detected also on Cerealia Facula. Moreover, Cerealia spectra are unusually

red-sloped between 0.4 and 1.0 μm (ref. [35]), a characteristic similar to the organic-rich terrains at Ernutet[36]. Spectral modelling of the average facula bright material using also terrestrial aliphatics, like those used to model Ernutet terrains[33,34], indicates an upper limit of 2% of organics, while aromatic hydrocarbons or organics with spectra like insoluble organic material[37,38] have an upper limit of 6–8%, with a marginal improvement of the fits (Extended Data Figs. 5 and 9).

Hydrohalite and the preservation of current fluids

The discovery of hydrated sodium chloride has implications in the preservation of brines as residua of an early ocean. In fact, according to thermal models, the preservation of a relict ocean until the present is possible if the crust contains a high abundance of insulating materials, such as hydrohalite[5]. Moreover, sodium and ammonium chloride lower the eutectic temperature of the brines. As a consequence, is conceivable that the salt content of Ceres could maintain brine-liquid pockets at present.

We wonder whether Occator-like geology and processes were common for other craters on Ceres in the past, or if there are other craters sharing similarity with Occator at the present. Several areas show sodium carbonates[20] as in Occator, with important exposure of these minerals in recent and ice-rich craters, such as Oxo crater[20], suggesting a possible correlation between the age of the craters and the exposure of brine residua that seems to fade with time. We cannot exclude that other older craters, similarly to Occator, have had brine extrusions, conveyed by conduits and fractures, but such exposures are now reworked, dispersed and covered by successive impacts.

Occator dome is geologically very recent[25] and possibly it is the result of active cryovolcanism, but there are also other potential cryovolcanic processes on Ceres. Ahuna Mons[13] and other mountains[11,12] have been interpreted as the results of cryovolcanism, with ascending fluids from the subsurface. However, in these cases, the fluids may not have been able to fully extrude on Ceres's surface, as in Occator. Nevertheless, some minerals, such as sodium carbonates, constituting briny fluids, are visible on the domes, specifically the bright streaks on the flank of Ahuna Mons[39], or in close proximity to them, as reported by ref. [20], reinforcing the hypothesis of cryovolcanism as an important process on Ceres.

The mineral assemblage found in Occator bright materials and its relation to the geologic features of the area suggests a recent or still ongoing complex hydrothermal system, characterized by the circulation of brines from subsurface sources containing hydrated sodium salts, sodium carbonates and ammonium chloride, in addition to the other aqueous altered material commonly found on Ceres. Moreover, the presence of organic material cannot be excluded and the hydrohalite, in association with evaporite minerals, could offer crystalline surfaces as adsorption sites, creating a favourable environment for catalysis, synthesis, concentration, polymerization and organization of prebiotic molecules.

Methods

Cerealia Facula morphology. The Cerealia Facula bright deposits are located in the central pit of Occator (14.7 km wide and 1 km deeper than the crater's floor), which hosts also the Cerealia Tholus dome at its centre (~3 km diameter, 0.34 km height) (Extended Data Fig. 1). The Pasola Facula deposits lay on a 1.5 by 0.5 km mesa located 3.6 km southwest from the central dome (Extended Data Fig. 2). The mesa is 600 m higher than the top of Cerealia Tholus and dips towards it with an average inclination of 22°. The brightness gradient within the Cerealia Facula deposits tends to darken as they near the contact with the surrounding materials at a radial distance of about 3.5 km. The contacts between Pasola Facula and the surrounding darker material are sharp (Extended Data Fig. 2).

The Cerealia Tholus dome is characterized by a series of radial fractures off-centred from the highest topographic point (Fig. 2). Cerealia Facula's boundaries to the darker materials of Occator's floor are characterized by a series of concentric fractures, interrupted in the southwestern sector by the Pasola Facula mesa, which has its long axis tangent to the pattern of fractures, which border Cerealia Facula. Both the concentric and the radial fractures show the morphology

of an extensional fault system[17]. The concentric fractures around Cerealia Facula have been interpreted as being generated during the collapse of the central pit. Many fractures and faults are found within the floor of Occator crater, some of which are concentric or radial to the central depression. Concentric troughs within crater floors typically have an extensional nature (normal fault systems). The eastern and western borders of the high-standing terrain of Pasola Facula are aligned concentrically to the crater centre. We argue that two main concentric normal faults that border the high-standing terrain were the cause of its uplift that behaved like a horst or semi-horst structure, which caused the displacement of Pasola Facula with respect to the Cerealia Facula border to the east. The presence of radial fractures is likely due to the formation of the central dome that could have been put in place with a lifting of the surface from below due to the emplacement of a mass in the subsurface or through the expansion of the volume of the subsoil through the freezing of a mass of water (viz. pingo).

Data analyses. We model Cerealia Facula spectra as an intimate mixture of different endmembers, by means of Hapke theory, which characterizes light scattering in particulate media. The abundance and grain size of the components are free parameters, and the best fit is obtained by means of a least-squares optimization algorithm[3,16]. The model accounts for the viewing geometry (incidence, emission and phase angle), which is calculated according to the shape model, the spacecraft attitude, and the latitude and longitude of a given pixel on the surface. The endmembers used in the fitting procedure are listed in Extended Data Fig. 7. Given the uncertainties on the possible presence of dark/neutral materials, we adopted a multiplicative constant to adjust the absolute level. We started the modelling using the bright spot composition derived in refs. [2,3]. As discussed in the main text, we added hydrated sodium carbonate or the brines derived in the experiments in ref. [22]. The retrieved abundances for the different fits, described in the main text and here, are in Extended Data Fig. 7. To check the presence of organics, we fitted the average spectra of Cerealia Facula using also organics spectra as described in Extended Data Fig. 9. The VIR data used in these analyses are reported in Extended Data Fig. 10. The details of the model are given in ref. [3].

Stability and dehydration of hydrohalite. We applied a three-dimensional finite-element-method thermophysical model to quantify the dehydration rate and the 'lifetime' of a hydrohalite layer in the Occator crater. The details of the model are given in ref. [26]. Here we use the model to roughly estimate the temperatures of the areas containing hydrohalite, also taking into account the self-heating between the facets of the mesh covering the crater. The real topography is here used to simulate the temperatures (Extended Data Fig. 6) and dehydration rate. A rotational matrix[40] is applied to the facets of the mesh to simulate the rotation of Ceres and the resulting insulation variability. We virtually put a 1-m-thick layer of hydrohalite at the centre of the crater. The physical parameters for the hydrohalite layer used in our simulations are the same as suggested by ref. [41] and used in the model of ref. [5]: density 2,200 kg m^{-3}, specific heat 920 J kg^{-1} K^{-1} and thermal conductivity 0.6 W m^{-1} K^{-1}. The albedo 0.24 is taken from ref. [42]. We calculate the rate of dehydration by using the classical formula for the sublimation of ice, given the similarity of the stability curves of the ice and hydrohalite[27]. Formally, we obtain an upper limit for the dehydration rate of hydrohalite. Hydrohalite dehydration would be slower than that of ice of about one order of magnitude (less than ten times slower than ice).

Several Ceres rotations are performed to reach a stationary state. Given the above assumptions, our simulations suggest that surface temperatures are in the range of 160–180 K. In this case, the estimated dehydration rate is in the range 10^{19}–10^{21} molecules s^{-2} m^{-2}. We note that this is a rough estimation, being calculated by using the mean temperature of the layer. We obtain that the lifetime of a 1-m-thick layer is of the order of tens to hundred of years; thus we foresee a rapid dehydration of the sodium chloride. We do not expect large deviations from these results if we use different thermal inertia or heliocentric distance. In Extended Data Fig. 6, we plot the temperature of the dome located at the centre of Occator, at different heliocentric distances—aphelion, perihelion and 2.70 au—as well as the dehydration rate and the three-dimensional reconstruction of Occator crater.

Data availability

Dawn data are archived in NASA's Planetary Data System. VIR spectral data may be obtained at https://sbn.psi.edu/pds/resource/dawn/dwncvirL1.html.

References

1. Scully, J. E. C. et al. Synthesis of the special issue: the formation and evolution of Ceres' Occator crater. *Icarus* **320**, 213–225 (2019).
2. De Sanctis, M. C. et al. Bright carbonate deposits as evidence of aqueous alteration on (1) Ceres. *Nature* **536**, 54–57 (2016).
3. Raponi, A. et al. Mineralogy of Occator crater on Ceres and insight into its evolution from the properties of carbonates, phyllosilicates, and chlorides. *Icarus* **320**, 83–96 (2019).

4. Russell, C. T. et al. Dawn arrives at Ceres: exploration of a small, volatile-rich world. *Science* **353**, 1008–1010 (2016).
5. Castillo Rogez, J. C. et al. Conditions for the long-term preservation of a deep brine reservoir in Ceres. *Geophys. Res. Lett.* **46**, 1963–1972 (2019).
6. Bland, M. T. et al. Composition and structure of the shallow subsurface of Ceres revealed by crater morphology. *Nat. Geosci.* **9**, 538–542 (2016).
7. Fu, R. R. et al. The interior structure of Ceres as revealed by surface topography. *Earth Planet. Sci. Lett.* **476**, 153–164 (2017).
8. Prettyman, T. H. et al. Extensive water ice within Ceres' aqueously altered regolith: evidence from nuclear spectroscopy. *Science* **355**, 55–59 (2017).
9. Combe, J.-P. et al. Detection of local H_2O exposed at the surface of Ceres. *Science* **353**, aaf3010 (2016).
10. Raponi, A. et al. Variations in the amount of water ice on Ceres' surface suggest a seasonal water cycle. *Sci. Adv.* **4**, eaao3757 (2018).
11. Sori, M. M. et al. The vanishing cryovolcanoes of Ceres. *Geophys. Res. Lett.* **44**, 1243–1250 (2017).
12. Sori, M. M. et al. Cryovolcanic rates on Ceres revealed by topography. *Nat. Astron.* **2**, 946–950 (2018).
13. Ruesch, O. et al. Cryovolcanism on Ceres. *Science* **353**, aaf4286 (2016).
14. Küppers, M. et al. Localized sources of water vapour on the dwarf planet (1) Ceres. *Nature* **505**, 525–527 (2014).
15. Ammannito, E. et al. Distribution of phyllosilicates on Ceres. *Science* **353**, aaf4279 (2016).
16. De Sanctis, M. C. et al. Ammoniated phyllosilicates with a likely outer Solar System origin on (1) Ceres. *Nature* **528**, 241–244 (2015).
17. Buczkowski, D. L. et al. Tectonic analysis of fracturing associated with Occator crater. *Icarus* **320**, 49–59 (2019).
18. Bowling, T. et al. Post-impact thermal structure and cooling timescales of Occator crater on asteroid 1 Ceres. *Icarus* **320**, 110–118 (2019).
19. De Sanctis, M. C. et al. The VIR spectrometer. *Space Sci. Rev.* **163**, 329–369 (2011).
20. Carrozzo, F. G. et al. Nature, formation, and distribution of carbonates on Ceres. *Sci. Adv.* **4**, e1701645 (2018).
21. Vu, T. H. et al. Preferential formation of sodium salts from frozen sodium–ammonium–chloride–carbonate brines—implications for Ceres' bright spots. *Planet. Space Sci.* **141**, 73–77 (2017).
22. Thomas, E. C. et al. Kinetic effect on the freezing of ammonium–sodium–carbonate–chloride brines and implications for the origin of Ceres' bright spots. *Icarus* **320**, 150–158 (2019).
23. Stein, N. et al. The formation and evolution of bright spots on Ceres. *Icarus* **320**, 188–201 (2019).
24. Quick, L. C. et al. A possible brine reservoir beneath Occator crater: thermal and compositional evolution and formation of the Cerealia Dome and Vinalia Faculae. *Icarus* **320**, 119–135 (2019).
25. Neesemann, A. et al. The various ages of Occator crater, Ceres: results of a comprehensive synthesis approach. *Icarus* **320**, 60–82 (2019).
26. Formisano, M. et al. Thermal stability of water ice in Ceres' craters: the case of Juling crater. *J. Geophys. Res.* **123**, 2445–2463 (2018).
27. Zolotov, M. Y. Aqueous origins of bright salt deposits on Ceres. *Icarus* **296**, 289–304 (2017).
28. Manga, M. & Wang, C. Y. Pressurized oceans and the eruption of liquid water on Europa and Enceladus. *Geophys. Res. Lett.* **34**, L07202 (2007).
29. Postberg, F. et al. A salt-water reservoir as the source of a compositionally stratified plume on Enceladus. *Nature* **474**, 620–622 (2011).
30. Waite, J. H. Jr et al. Cassini ion and neutral mass spectrometer: Enceladus plume composition and structure. *Science* **311**, 1419–1422 (2006).
31. Waite, J. H. Jr et al. Liquid water on Enceladus from observations of ammonia and ^{40}Ar in the plume. *Nature* **460**, 487–490 (2009); corrigendum **460**, 1164 (2009).
32. Postberg, F. et al. Macromolecular organic compounds from the depths of Enceladus. *Nature* **558**, 564–568 (2018).
33. De Sanctis, M. C. et al. Localized aliphatic organic material on the surface of Ceres. *Science* **355**, 719–722 (2017).
34. De Sanctis, M. C. et al. Characteristics of organic matter on Ceres from VIR/Dawn high spatial resolution spectra. *Mon. Not. R. Astron. Soc.* **482**, 2407–2421 (2019).
35. Natheus, A. et al. Occator crater in color at highest spatial resolution. *Icarus* **320**, 24–38 (2019).
36. Pieters, C. M. et al. Geologic constraints on the origin of red organic-rich material on Ceres. *Meteorit. Planet. Sci.* **53**, 1983–1998 (2018).
37. Moroz, L. V. et al. Natural solid bitumens as possible analogs for cometary and asteroid organics: 1. reflectance spectroscopy of pure bitumens. *Icarus* **134**, 253–268 (1998).
38. Kaplan, H. H. et al. New constraints on the abundance and composition of organic matter on Ceres. *Geophys. Res. Lett.* **45**, 5274–5282 (2018).
39. Zambon, F. et al. Spectral analysis of Ahuna Mons from Dawn mission's visible-infrared spectrometer. *Geophys. Res. Lett.* **44**, 97–104 (2017).
40. Formisano, M. et al. Surface temperatures and water ice sublimation rate of Oxo crater: a comparison with Juling crater. *J. Geophys. Res.* **124**, 2–13 (2019).
41. Schofield, N. et al. Mobilizing salt: magma–salt interactions. *Geology* **42**, 599–602 (2014).
42. Li, J.-Y. et al. Surface albedo and spectral variability of Ceres. *Astrophys. J. Lett.* **817**, L22 (2016).

Acknowledgements

Author contributions

M.C.D.S. elaborated interpreted VIR data, and wrote most of the manuscript. A.F. elaborated the VIR data projections over FC data. A.R. developed the spectral modelling of the spectra. M. Formisano developed the thermal model. All authors participated in data acquisition, discussion of results and/or editing of the manuscript.

Competing interests

Additional information
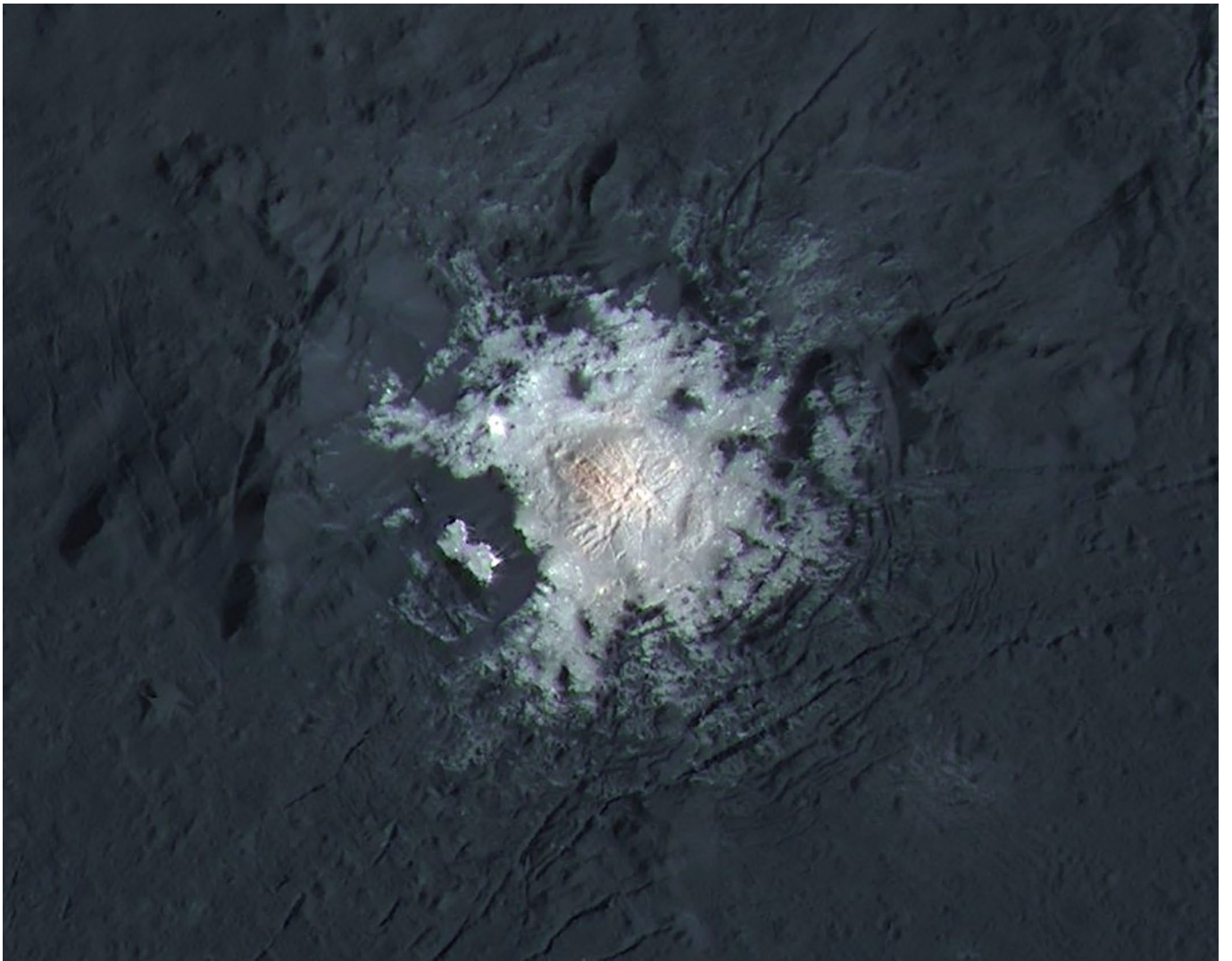
Extended Data Fig. 1 | Cerealia Facula. Pan-sharpened FC colour data showing an asymmetric distribution of reddish material (NASA/JPL-Caltech/ UCLA/MPS/DLR/IDA).
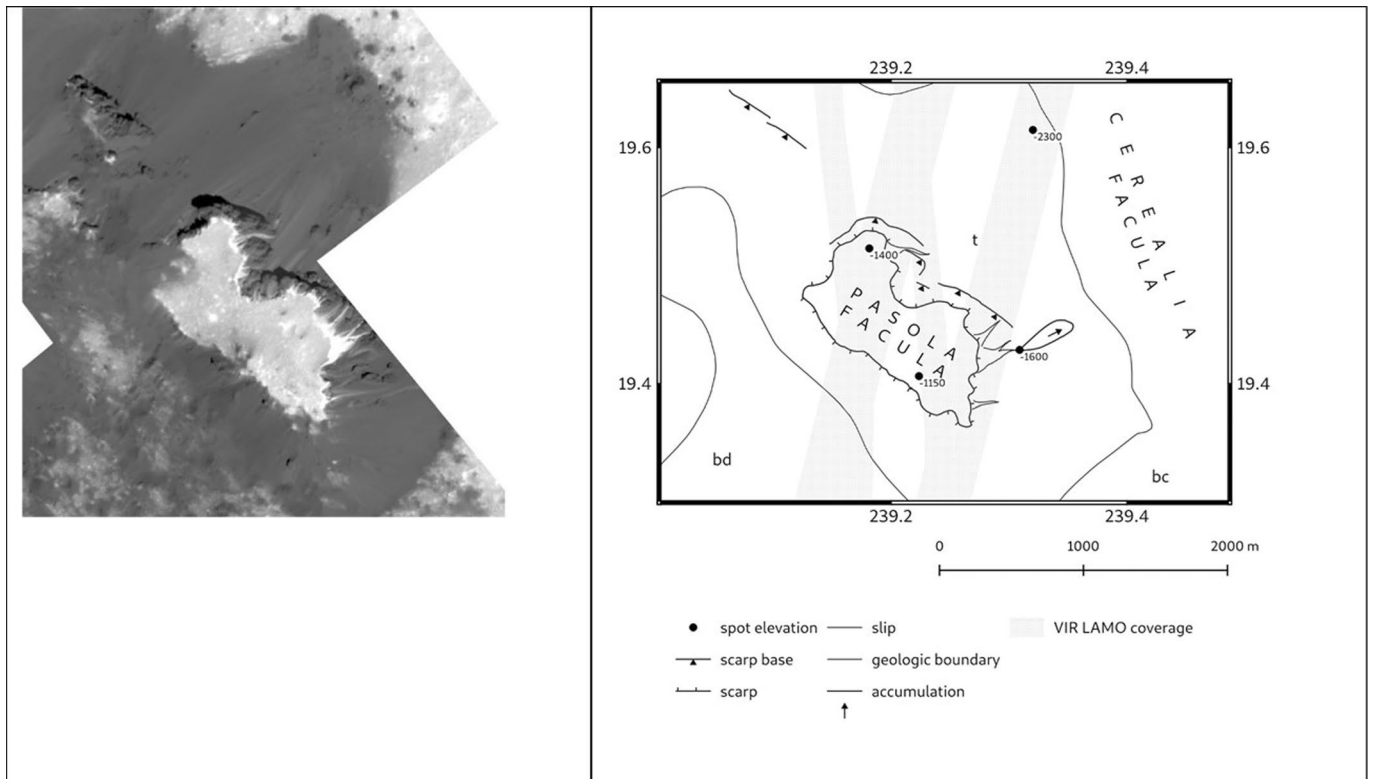
Extended Data Fig. 2 | Pasola Facula. Pasola Facula. Left) mosaic of Pasola facula located on the western side of Cerealia Facula (NASA/JPL-Caltech/ UCLA/MPS/DLR/IDA); Right): Map of Pasola Facula showing VIR coverage (in grey) along with the main geologic features. Units label are: bd, the bright discontinuous unit – bc, bright continuous unit and t, talus material.

**Extended Data Fig. 3 | A typical spectrum of Cerealia facula.** An example of spectra of Cerealia facula with highlighted the main features within the 2.6–3.5 micron band.
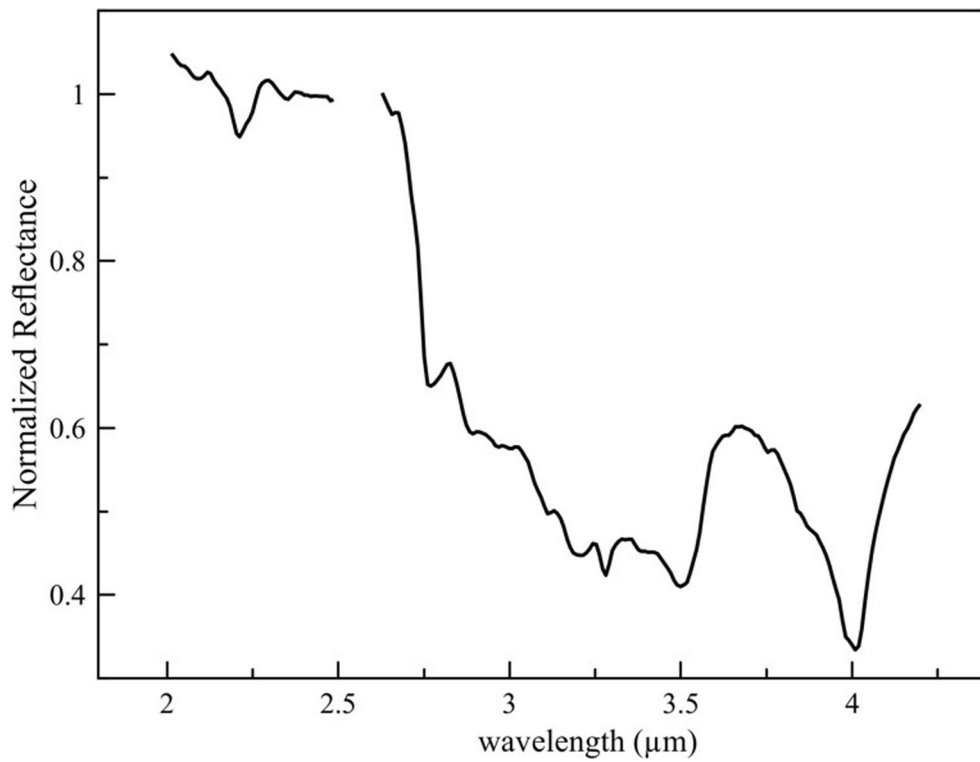
Extended Data Fig. 4 | Spectrum of the southern part of Pasola Facula. Average spectrum of the pixels covering the southern part of Pasola Facula. The data at 2.5 micron has been removed because affected by the detector filters.
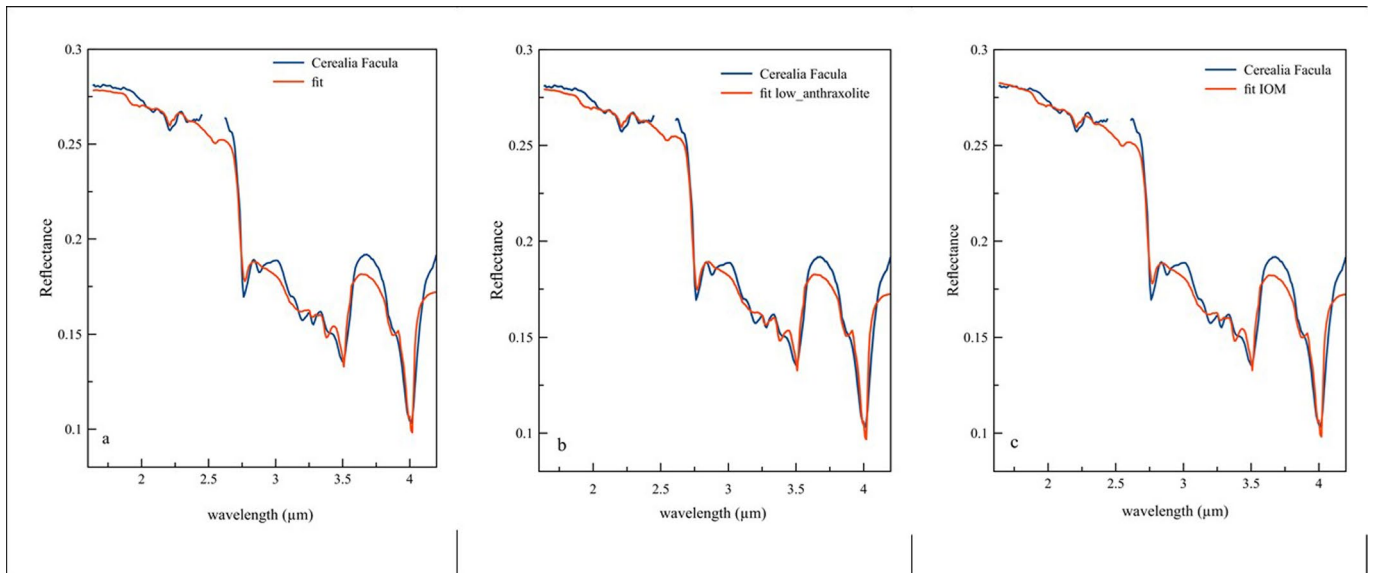
Extended Data Fig. 5 | Spectral fits of the average spectrum of Cerealia facula. The spectrum used for the spectral modelling is an average of the spectra of the pixels on the bright Cerealia facula selected on the basis of the absolute reflectance (median reflectance > 5 times median reflectance of dark surrounding regions, in the range 2.6 – 3.4 μm). Dataset used is described in Extended Data Table 4. A) spectral fit using the species reported in Extended Data Table 3, without organics; B) spectral fit using the species reported in Extended Data Table 3, including low-anthraxolite; C) spectral fit using the species reported in Extended Data Table 3, including IOM. The data 2.5 micron has been removed because affected by the detector filters.
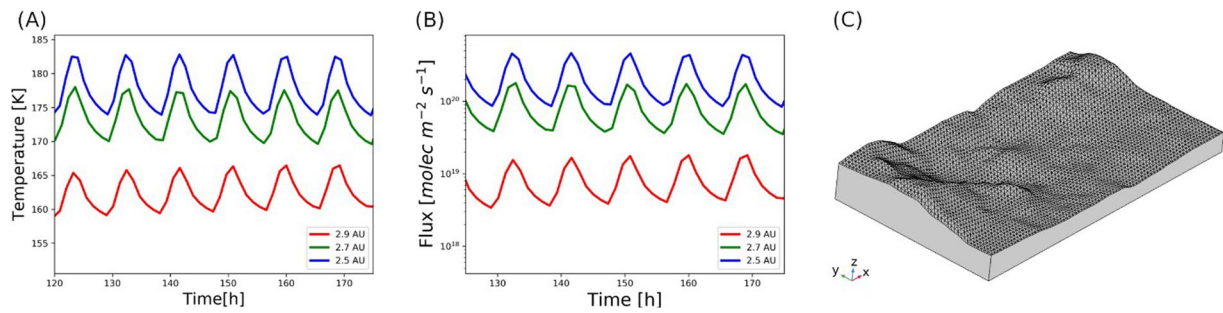
Extended Data Fig. 6 | Thermal models of the hydrohalite rich area. a) Temperature of the hydrohalite rich region, located at the centre of Occator, at different heliocentric distances: aphelium, perihelium and 2.70 AU; B) Dehydration rate on Occator at same heliocentric distances; C) 3-D reconstruction of Occator used in our numerical modelling.

End Member Sample id/ Reference	Mineral (%)	Fig. a	Fig. b	Fig. c
Thomas et al.	Sol.3 (%)	-	-	27
CB-EAC-034-A	trona (%)	-	20	-
CB-EAC-034-C	natrite (%)	36	44	38
CB-EAC-003	dolomite (%)	0	7	5
CL-EAC-049-A	ammonium chloride (%)	9	6	1
IL-EAC-001	illite (%)	17	12	11
MG-EAC-002	dark material* (%)	38	11	18
	Grain size (µm)	125	20	38
	X^2	5.08	2.67	1.57

*magnetite.

Extended Data Fig. 7 | Spectral modelling. Species used in the spectral fits, retrieved abundance and X^2 of the spectral modelling. The percentage are expressed in cross section (% of surface). The end member spectra are taken form RELAB except for Sol.3 from 22. The spectrum used for the fits is the average of the spectra of samples 61-64, line 82, scet 582998159.

Species	Solution 1	Solution 2	Solution 3
	(equimolar Na$^+$ and NH$_4$$^+$)	*(dominant NH$_4$$^+$)*	*(dominant Na$^+$ or Cl$^-$)*
NH$_4$Cl	X	X	X
NH$_4$HCO$_3$	X		
NaHCO$_3$			
NaCl 2H$_2$O			X
Na$_2$CO$_3$	X	X	X

Extended Data Fig. 8 | Species present in frozen ammonium-sodium-chloride-carbonate brine mixtures. Species present in frozen ammonium-sodium-chloride-carbonate brine mixtures from ref. [22]. Solution 1 was prepared with an equal amount of sodium and ammonium ions. Solution 2 was prepared at room temperature and was composed of 0.6 M [Na$^+$], 3.6 M [NH$_4$$^+$], 3.6 M [Cl$^-$], and 0.3 M [CO$_3$$^{2-}$]. Solution 3 was prepared at room temperature and composed of 3.1 M [Na$^+$], 0.6 M [NH$_4$$^+$], 3.1 M [Cl$^-$], and 0.3 M [CO$_3$$^{2-}$]. See ref. [22] for details.

Sample id/ Reference	mineral	Fit a	Fit b	Fit c
Moroz et al. 1998	High_kerite/ low_anthraxolite (%)	-	6	-
Kaplan et al 2018	Murchison IOM (%)	-	-	8
Thomas et al. 2019	Sol.3	13	12	14
CB-EAC-034-C	natrite (%)	56	56	54
CB-EAC-003	dolomite (%)	3	2	3
CL-EAC-049-A	ammonium chloride (%)	0	0	0
IL-EAC-001	illite (%)	20	24	21
MG-EAC-002	dark material* (%)	8	0	0
	Grain size (µm)	*13*	*11*	*14*
	X^2	**1.55**	**1.47**	**1.52**

*magnetite.

Extended Data Fig. 9 | Spectral modelling of the brightest pixels, including organic species. Species used in the spectral fits, retrieved abundance and X^2 of the spectral modelling. The spectrum used for the spectral modelling is an average of the spectra of the pixels on the bright Cerealia facula selected on the basis of the absolute reflectance (median reflectance > 5 times median reflectance of dark surrounding regions, in the range 2.6 – 3.4 µm). The percentage are expressed in cross section (% of surface). Dataset used is described in Extended Data Fig. 10.

Spacecraft clock start count	Acquisition time	Resolution across slit (m/px)	Phase angle (°) ± 0.25°
584957323	2018-07-15	18.485	42.2
582998159	2018-06-23	9.183	40.0
521436704	2016-07-10	95.420	38.3
509021651	2016-02-17	90.363	47.2

Extended Data Fig. 10 | VIR data used in the spectral modelling. VIR infrared data used in this analysis.